

# Intensity correlation and anticorrelations in coherently prepared atomic vapor

Gombojav O. Ariunbold<sup>1,4,\*</sup>, Vladimir A. Sautenkov<sup>1,3</sup>, Yuri V. Rostovtsev<sup>1</sup>, and Marlan O. Scully<sup>1,2</sup>

<sup>1</sup>*Institute for Quantum Studies and Department of Physics,  
Texas A & M University, College Station, Texas 77843, USA*

<sup>2</sup>*Department of Aerospace and Mechanical Engineering,  
Princeton University, Princeton, New Jersey 08544, USA*

<sup>3</sup>*Lebedev Institute of Physics, Moscow 119991, Russia*

<sup>4</sup>*Theoretical Physics Laboratory, National University of Mongolia, 210646 Ulaanbaatar, Mongolia*

(Dated: July 30, 2018)

Motivated by the recent experiment [V.A. Sautenkov, Yu.V. Rostovtsev, and M.O. Scully, Phys. Rev. A 72, 065801 (2005)], we develop a theoretical model in which the field intensity fluctuations resulted from resonant interaction of a dense atomic medium with laser field having finite bandwidth. The intensity-intensity cross correlation between two circular polarized beams can be controlled by the applied external magnetic field. A smooth transition from perfect correlations to anti-correlations (at zero delay time) of the outgoing beams as a function of the magnetic field strength is observed. It provides us with the desired information about decoherence rate in, for example, <sup>87</sup>Rb atomic vapor.

PACS numbers: 32.80.Qk, 42.50.Ar

## I. INTRODUCTION

The fundamental limits of spectral resolution and sensitivity of spectroscopic techniques, the information transfer and computation rates, spatial resolution of optical microscopy and imaging are determined by statistical properties of light. For the last five decades enormous theoretical and experimental research activities have been devoted to studying fluctuations in classical and quantum systems [1].

The first experiment on the correlation between the intensity fluctuations recorded at the two different photo-detectors illuminated by the same thermal light source was performed by Hanbury-Brown and Twiss [2]. In their experiment, photon bunching, i.e., an enhancement in the intensity-intensity correlations has been observed.

Quantum formulation of optical coherences was introduced by Glauber in his pioneering work [3]. Photon anti-bunching has been predicted by Carmichael et al. [4] and then it was firstly observed in resonance fluorescence experiment by Kimble et al. [5].

As a generalization of the results obtained for two-level atomic systems [6, 7] to fluorescence from a  $\Lambda$  three-level atomic system showing an anti-bunching effect in the second order correlations has been studied in [8]. Due to four-wave mixing in cold atoms [9] under condition of electromagnetically induced transparency (EIT) [10], Harris and co-workers [11] have measured the correlation between Stokes and anti-Stokes photons emitted from Rb atoms with short time delay.

Kuzmich et al. [12] have demonstrated a generation of pair photons with controllable time delay in the issue of quantum information storage and retrieval [13, 14] using ensemble of atoms [15]. The correlated photons have been greatly attracted in the study of, e.g., entanglement amplifier [16], subnatural spectroscopy [17], quantum microscopy [18], nonclassical imaging of trapped ions [19]

and many others.

A transition from anti-bunching to bunching of light emitted from a few atoms in a very high finesse cavity has been demonstrated [20]. The transition occurs by increasing a number of atoms interacting with light [21].

The matched fields treated both classically [22] and quantum mechanically [23] can be another promising theoretical approach to the switching of correlations in a three-level atomic sample. However, the result is very sensitive to the detuning between driven fields and atomic levels. Photon bunching in the intensity-intensity correlations between pump and probe fields for different probe detunings in Rb vapor [26] and in the temporal correlations between forward and backward anti-Stokes photons scattered from sodium vapor [27] has been demonstrated.

The most recently, Scully and co-workers [28] have obtained a smooth transition from EIT correlated to anti-correlated photons emitted from coherently prepared <sup>87</sup>Rb vapor.

In the present work we develop a theory to explain the results of the previous experiments [28], whereas laser source to be considered here with a finite bandwidth. A diode laser used in our experiment, would have low intensity fluctuations but non-negligible phase fluctuations under certain condition. The fluctuations of the input light after interacting with the atomic sample can be enhanced and contain information about atomic sample. For instance, this has been used as a spectroscopic tool [29, 30]. Particularly, the laser phase fluctuations can be converted into the intensity fluctuations due to the interaction of field with atomic vapor [31, 32, 33, 34].

Furthermore, based on the numerical results, we suggest a new promising method to estimate decoherence rate for Zeeman sub-levels.

This paper is organized as follows. In the next section, the experimental setup is described and the obtained re-

sults are reported. In section III, we study the absorption induced fluctuations of laser beam intensities and their correlations by considering a generic three-level  $\Lambda$  atomic system interacting with laser fields with orthogonal polarizations. We obtain the approximate analytical solutions elucidating an origin of perfect correlations as well as anti-correlations between two modes. Then, in the next section, we solve numerically equations of motion to prove the results of the analytical predictions. The last section is conclusion.

## II. EXPERIMENTAL SETUP AND OBTAINED RESULTS

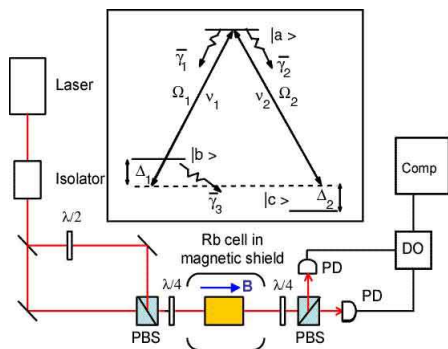


FIG. 1: A simplified schematics of experimental setup and a level scheme considered for Rb atoms. PBS: polarizing beam-splitter,  $\lambda/2$ ,  $\lambda/4$ : wave plates, PD: photo-detector, DO: digital oscilloscope, Comp: computer.

A setup of the experiment (similar to one in [28]) is shown in Fig. 1. An external-cavity diode laser [35] is tuned to  $D_1$  line ( $5S_{1/2}(F = 2) \leftrightarrow 5P_{1/2}(F' = 1)$ ) of  $^{87}\text{Rb}$ . An input beam is separated by a beam-splitter. The polarizations of these two separated beams become orthogonal using a  $\lambda/2$ -wave plate put on the way of one beam and these are combined together by a polarizing beam-splitter (PBS). After the  $\lambda/4$  wave-plate the beam is a combination of two circular polarized optical fields. A glass cell of length  $L = 7.5\text{cm}$  with Rb vapor (natural abundance) at density approximately  $10^{12}\text{cm}^{-3}$  is installed in a two-layer magnetic shield. A simplified level scheme is depicted in inset of Fig. 1. The opposite circular polarized beams interact with the vapor and induce a ground state Zeeman coherence in Rb atoms. EIT resonance is presented in Fig. 2. Transmitted laser beams after the second  $\lambda/4$  wave-plate are separated again by another polarizing beam-splitter and focused on fast photodiodes (PD) with frequency bandwidth  $75\text{kHz}-1.2\text{GHz}$ . The optical path lengths for both beams are the same. Signals from PDs are sent to a digital oscilloscope (DO). As varying a magnitude of longitudinal magnetic field the transmitted fields are changed at the optical power of  $0.5\text{mW}$  (total power  $1\text{mW}$ ) and beam diameter of  $0.1\text{cm}$  for each beam at the entrance window of the Rb cell.

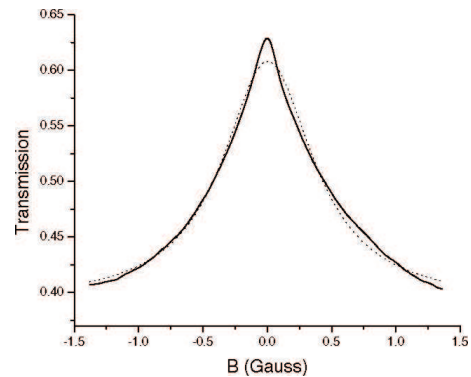


FIG. 2: A transmission of the optical field through the Rb cell as a function versus magnetic field  $B$  (solid curve). Dots stand for Lorentzian fit. The total optical power at all at entrance window is  $1\text{mW}$ .

The time dependent intensity fluctuations  $\delta I_{1,2}(t)$  of both

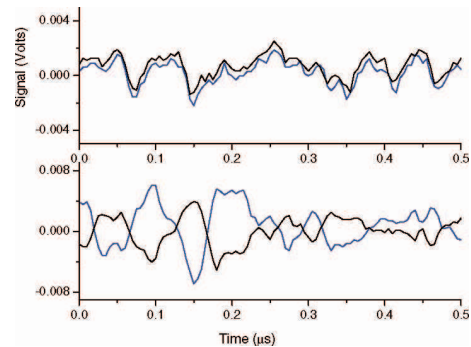


FIG. 3: Waveforms from photo-detectors with total optical power of laser beams at front window of Rb cell is  $1\text{mW}$ . The fluctuations of intensities versus time for two coinciding beams with (a) no magnetic field  $B = 0$  and (b) applied magnetic field  $B = -0.47\text{Gauss}$ .

optical beams transmitted through Rb vapor, are registered by the photodetectors (see, Fig. 3). Data presented here is a part of the recorded data in  $10\mu\text{sec}$ . The signal in Volts is proportional to laser intensity as  $500\text{V/W}$ . Furthermore, the intensity-intensity correlations between two modes can be calculated using the observed data for the intensity fluctuations. The second order correlation function  $G^{(2)}(\tau)$  for intensity fluctuations of two optical beams with time delay  $\tau$  is given by

$$G^{(2)}(\tau) = \frac{\langle \delta I_1(t) \delta I_2(t + \tau) \rangle}{\sqrt{\langle [\delta I_1(t)]^2 \rangle \langle [\delta I_2(t + \tau)]^2 \rangle}} \quad (1)$$

where the time average of arbitrary variable  $Q(t)$  is defined as  $\langle Q(t) \rangle = \int_t^{t+T} Q(t) dt / T$ . The integration time  $T$  is taken to be as large as  $10\mu\text{s}$ . In the absence of the external magnetic field  $B = 0$  where EIT condition is fulfilled (two-photon detuning is zero), the induced fluctuations

of the transmitted beams by Rb vapor are almost synchronized (see Fig. 3(a)). In the case of zero detuning, the intensity-intensity correlation curve of Fig. 4(a) has a sharp spike clearly showing bunching. The magnitude of the correlation peak at  $\tau = 0$  is of 0.9 and the average background is near 0.15. The width of the correlation peak increased as reduces the optical power. On the other hand, the most intriguing feature is observed when an applied magnetic field is of  $B = -0.47$ Gauss. As is seen from Fig. 3(b), intensity fluctuations are out of phase when two photon detuning becomes non zero. A presence

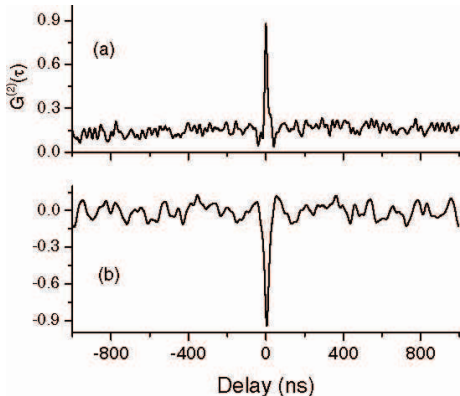


FIG. 4: Intensity-intensity correlation functions  $G^{(2)}(\tau)$  as functions of time delay  $\tau$  for magnetic fields  $B = 0$  (above) and  $B = -0.47$  (bottom).

of the magnetic field demonstrates an exhibition of anti-correlation (see Fig. 4(b)) as is expected from the data plotted in Fig. 3(b). The width of the peaks is associated with the saturated width of resonance in Rb vapor absorption (a single photon resonance) [36]. Moreover, the second order correlation  $G^{(2)}(\tau)$  obtained with spatially separated beams (distance between beams 0.3cm which is bigger than the beam diameter 0.1cm) has a correlation peak (at  $\tau = 0$ ) of 0.7 and a larger background of 0.3. This contrast indicates that the enhanced correlations are clearly due to overlap of two beams. We have also performed a set of measurements of  $G^{(2)}(\tau = 0)$  for different values of the magnetic field  $B$  at optical power 1mW (see, Fig. 10). A measurement shows that a perfect switching from photon correlation to anticorrelation where the correlation peak with magnitude 0.9 for zero magnetic field  $B = 0$  switches to a dip with magnitude  $-0.9$  for  $B = -0.47$ Gauss. This pronounced modification of waveforms is very important in determination of some experimental parameters which will be shown later. The width related to intensity-intensity correlations  $G^{(2)}(\tau = 0)$  are 0.24Gauss, almost four times narrower than the corresponding EIT width which is 0.85Gauss for optical power 1mW.

### III. THEORETICAL RESULTS

#### A. Three-level $\Lambda$ atoms driven by laser with finite bandwidth

Let us consider interaction of two modes generated by the diode laser with three-level  $\Lambda$  atoms that have a level scheme shown in Fig. 1. The equations of motion for this system are given by (e.g. see [8])

$$\begin{aligned}
 \dot{\rho}_{bc} &= -(\gamma_3 + i\Delta)\rho_{bc} + i\Omega_1\rho_{ca}^\dagger - i\Omega_2\rho_{ba} \\
 \dot{\rho}_{ba} &= -(\gamma_1 + i\Delta_1)\rho_{ba} - i\Omega_1(\rho_{bb} - \rho_{aa}) \\
 &\quad - i\Omega_2\rho_{bc} + i\dot{\phi}(t)\rho_{ba} \\
 \dot{\rho}_{ca} &= -(\gamma_2 - i\Delta_1)\rho_{ca} - i\Omega_2(\rho_{cc} - \rho_{aa}) \\
 &\quad - i\Omega_1\rho_{bc}^\dagger + i\dot{\phi}(t)\rho_{ca} \\
 \dot{\rho}_{bb} &= \tilde{\gamma}_3\rho_{cc} + \tilde{\gamma}_1\rho_{aa} + i\Omega_1\rho_{ba}^\dagger - i\Omega_1\rho_{ba} \\
 \dot{\rho}_{cc} &= \tilde{\gamma}_2\rho_{aa} - \tilde{\gamma}_3\rho_{cc} - i\Omega_2\rho_{ca} + i\Omega_2\rho_{ca}^\dagger
 \end{aligned} \tag{2}$$

where  $\rho_{aa} = 1 - \rho_{bb} - \rho_{cc}$ . The single and two photon detunings are  $\Delta_1 = \omega_a - \omega_c - \nu_2 = \nu_1 - \omega_a + \omega_b$ , ( $\nu_1 = \nu_2$ ) and  $\Delta = \omega_b - \omega_c$ . The effective decay parameters defined [37] as  $\gamma_3 = (\tilde{\gamma}_3 + \tilde{\gamma}_{21} + \tilde{\gamma}_{12})/2$ ,  $\gamma_1 = (\tilde{\gamma}_1 + \tilde{\gamma}_2 + \tilde{\gamma}_{21} + \tilde{\gamma}_{31})/2$  and  $\gamma_2 = (\tilde{\gamma}_1 + \tilde{\gamma}_2 + \tilde{\gamma}_3 + \tilde{\gamma}_{12} + \tilde{\gamma}_{32})/2$ , where  $\tilde{\gamma}_1$  and  $\tilde{\gamma}_2$  correspond to the spontaneous emission rates from level  $|a\rangle$  to levels  $|c\rangle$  and  $|b\rangle$ , respectively;  $\tilde{\gamma}_{21}$ ,  $\tilde{\gamma}_{12}$ ,  $\tilde{\gamma}_{32}$  and  $\tilde{\gamma}_{31}$  stand for dephasing rates, and  $\tilde{\gamma}_3$  is population decay rate of the level  $|b\rangle$ . In derivations of Eq.(2), we have kept the operator normal ordering, i.e., we neglect rapidly oscillating terms [6] and used re-scaled variables as  $\rho_{ij} \rightarrow 1/N_c\rho_{ij}$ ,  $N_c$  is number of collective atoms. A diode laser radiation experiences phase diffusion, and the phase  $\phi(t)$  in Eq.(2) represents the fluctuating phase [7] of driven field which is characterized by Wiener-Levy diffusion process [38]. For such process average and two-time correlation function of stochastic variables are given by

$$\begin{aligned}
 \overline{\langle \dot{\phi}(t) \rangle} &= 0 \\
 \overline{\langle \dot{\phi}(t)\dot{\phi}(t') \rangle} &= 2D\delta(t-t')
 \end{aligned} \tag{3}$$

where  $D$  is the diffusion coefficient; the stochastic averages denoted by the upper bar. Thus, the input laser field has a Lorentzian spectrum with a FWHM bandwidth of  $D/\pi$ Hz. In a realistic situation, the phase correlation has a finite relaxation time. The Gaussian process in which the correlations are determined by the exponential function of time delay is often referred to as Ornstein-Uhlenbeck [39] or colored noise. A stationary equation after taking stochastic average of Eq.(2) is shown in Appendix. The numerical simulations of Eq.(2) will be presented below.

## B. Absorption induced intensity-intensity correlations

Propagation equations for the laser fields are given by

$$\frac{\partial \Omega_1}{\partial z} = i\kappa_1 \rho_{ab}, \quad \frac{\partial \Omega_2}{\partial z} = i\kappa_2 \rho_{ac}. \quad (4)$$

In order to give a qualitative theoretical analysis of our experimental results, let us adopt a theory which implies for a thin absorbing medium. It is assumed that the transmitted field could be understood as a superposition of input and induced fields in the first order approximation for  $\kappa_{1,2}L$ , if  $\kappa_{1,2}L \ll 1$ ; here  $L$  is the length of the atomic sample and  $\kappa_{1,2}$  are some coefficients [30]. Furthermore, this could be still valid for a preferably long medium with a weak absorption, but satisfying the condition  $\kappa_{1,2}L \ll 1$ . In what follows, we will show that this approximation reproduces the observed results qualitatively. Following Walser et al. [30] and Martinelli et al. [34], the transmitted fields are given by

$$\begin{aligned} \Omega_1^{out}(t) &\approx \Omega_1 + i(\kappa_1 L) \rho_{ac}(t), \\ \Omega_2^{out}(t) &\approx \Omega_2 + i(\kappa_2 L) \rho_{ab}(t). \end{aligned} \quad (5)$$

To include Doppler effect, the coherence terms in Eq.(5) should be averaged by the Maxwell-Boltzmann velocity distribution. However, the Doppler broadening may play important role in many other experiment with Rb atomic vapor, but, in this case, it turns out not to be so crucial, because we are interested only in correlation behaviour as functions of two-photon detuning, instead of one-photon detuning. The transmitted intensities  $I_{1,2}(t) \Rightarrow |\Omega_{1,2}^{out}(t)|^2$  are, thus, written as

$$\begin{aligned} I_1(t) &\approx \Omega_1^2 + \Omega_1(\kappa_1 L) \text{Im}\{\rho_{ac}(t)\} \\ I_2(t) &\approx \Omega_2^2 + \Omega_2(\kappa_2 L) \text{Im}\{\rho_{ab}(t)\}. \end{aligned} \quad (6)$$

here  $\rho_{aq}$  is the atomic coherence term for level  $a$  and  $q$ , ( $q = b, c$ ) and we assume that the input fields are real and much stronger than the induced ones. Defining that  $\delta Q(t) = Q(t) - \overline{Q(t)}$  stands for the fluctuation of arbitrary variable  $Q(t)$ , the intensity fluctuation to be read

$$\begin{aligned} \delta I_1(t) &= \Omega_1(\kappa_1 L) \text{Im}\{\delta \rho_{ac}(t)\} \\ \delta I_2(t) &= \Omega_2(\kappa_2 L) \text{Im}\{\delta \rho_{ab}(t)\}. \end{aligned} \quad (7)$$

From this expression, it is easy to check that  $\langle \delta I_{1,2}(t) \rangle = 0$ , because  $\langle \delta \rho_{aq}(t) \rangle = 0$ ,  $q = c, b$ . From Eq.(7), using the definition Eq.(1) one obtains the intensity-intensity correlations

$$G^{(2)}(\tau) = \frac{\langle \text{Im}\{\delta \rho_{ac}(t)\} \text{Im}\{\delta \rho_{ab}(t+\tau)\} \rangle}{\sqrt{\langle [\text{Im}\{\delta \rho_{ac}(t)\}]^2 \rangle \langle [\text{Im}\{\delta \rho_{ab}(t)\}]^2 \rangle}} \quad (8)$$

The undertaking process is stationary, thus, the argument  $t+\tau$  of the last term in the denominator is displaced by  $t$ .

## C. Approximate theoretical analysis

### Zero detuning

Let us consider the resonant case where all detunings are set to be zero and  $\Omega_1 = \Omega_2$ ,  $\tilde{\gamma}_3 = 0$ ,  $\gamma_1 = \gamma_2$ . It is easy to show analytically that  $\langle \bar{\rho}_{bc} \rangle = \langle \bar{\rho}_{cb} \rangle$  where an equation for stationary state  $\bar{\rho}_{bc}$  is given in Appendix. According to exact numerical simulations of Eq.(2), the coherence term  $\rho_{bc}$  are real i.e.,  $\rho_{bc} \cong \rho_{bc}^\dagger$ . Therefore, equations for coherence terms  $\rho_{ba}$  and  $\rho_{ca}$  can have symmetrical forms as

$$\begin{aligned} \dot{\rho}_{ba} &= -\gamma_1 \rho_{ba} - i\Omega_1(\rho_{bb} - \rho_{aa}) + i\dot{\phi}(t)\rho_{ba} - i\Omega_1 \rho_{bc} \\ \dot{\rho}_{ca} &= -\gamma_1 \rho_{ca} - i\Omega_1(\rho_{cc} - \rho_{aa}) + i\dot{\phi}(t)\rho_{ca} - i\Omega_1 \rho_{bc} \end{aligned} \quad (9)$$

From Eq.(9), one can see that two equations, thus, two modes are decoupled. Note that because of symmetrical atomic configuration, it is obvious that populations  $\rho_{bb}$  and  $\rho_{cc}$  are identical  $\rho_{bb} \approx \rho_{cc}$ . This is, of course, true only in a resonant case. From Eq.(9), it follows that

$$\rho_{ba}(t) \approx \rho_{ca}(t) \quad (10)$$

This correlated behavior could be understood as follows. Phase fluctuations of incident beams are converted into intensities fluctuations via atom-field interactions as is seen from Eq.(2). Roughly speaking, the three-level atoms would experience driven fields with the effective Rabi frequencies fluctuating around  $\Omega_1$  which is resonant to the degenerate lower levels. Because the noise contribution is the same in two modes, any instant deviations from the resonance condition will be also the same. Thus, the induced absorption should be also the same for both modes. In this sense, this system would be in close relation to what is called a correlated emission laser firstly proposed by Scully [1], in which pairs of induced photons of different modes can be generated simultaneously exhibiting a sharp bunching.

### Non-zero detuning

In the non-degenerate situation, the equations for two modes are coupled. However, the effective Rabi frequencies would have again the same fluctuations, but,  $\Omega_1$  is no longer resonant to the lower levels. The induced absorption should not be the equivalent in this case, because, the deviations of the effective Rabi frequencies would become farther from one of ground levels, but, closer to another at any instant time. As a consequence, the populations of the excited and ground states would also fluctuate. By virtue of  $\dot{\rho}_{bb} + \dot{\rho}_{cc} \approx 0$ , since  $\dot{\rho}_{aa} \approx 0$ , it is possible to do the following assumption as

$$\begin{aligned} \rho_{bb}(t) &= c + f(t), \\ \rho_{cc}(t) &= c - f(t). \end{aligned} \quad (11)$$

where a fluctuation  $f(t)$  is real and  $c$  is constant. Note that it is not necessary to know an explicit expression for  $f(t)$ . This coupling function  $f(t)$  appears only because of non-zero detuning, otherwise it is zero. The equations for two polarizations,  $\rho_{ba}$  and  $\rho_{ca}$ , are given by

$$\begin{aligned}\dot{\rho}_{ba} &= -(\gamma_1 + i\Delta_1)\rho_{ba} - i\Omega_1 f(t) + i\dot{\phi}(t)\rho_{ba} - i\Omega_1\rho_{bc} + c' \\ \dot{\rho}_{ca} &= -(\gamma_1 - i\Delta_1)\rho_{ca} + i\Omega_1 f(t) + i\dot{\phi}(t)\rho_{ca} - i\Omega_1\rho_{bc}^\dagger + c'\end{aligned}\quad (12)$$

The formal solutions to be read

$$\begin{aligned}\rho_{ba}(t) &\sim +\Phi(t) + c_1 \\ \rho_{ca}(t) &\sim -\Phi(t) + c_2\end{aligned}\quad (13)$$

where  $\Phi(t) = -i\Omega_1 \int_{t_0}^t dt' e^{-\gamma_1(t-t') + i(\phi(t) - \phi(t'))} f(t')$ ,  $c_{1,2} = -i\Omega_1 \int_{t_0}^t dt' e^{-\gamma_1(t-t') + i(\phi(t) - \phi(t'))} (\rho_{bc,cb} + c)$  which can be slowly varying for  $t_0 \Rightarrow -\infty$ ,  $t \Rightarrow \infty$ . Note that, contributions of  $\Delta_1$  to solutions are neglected since, later on, only imaginary part of amplitudes will be of interest. Eq.(13) clearly indicates an exhibition of anti-correlation between two modes.

#### D. Numerical results

In the Ornstein-Uhlenbeck process [39], the colored noise  $\xi(t)$  yields the steady-state correlation function

$$\overline{\langle \xi(t)\xi(t') \rangle} = \Theta \lambda_L e^{-\lambda_L |t-t'|} \quad (14)$$

with  $\langle \xi(t) \rangle = 0$ . The stochastic differential equation Eq.(2) can be solved using Monte-Carlo numerical simulations. A Box-Mueller algorithm and the Euler-Maruyama method are used to realize the colored noise. Namely, one can see that the generated noise by the fast, integral algorithm developed in [40], is in a perfect agreement with the analytical definition given by Eq.(14) due to averaging over as many as 1000 different realizations. A relaxation time  $1/\lambda_L$  is taken to be small, to ensure that undertaking process would be approximately white noise, i.e.,  $\xi(t) \sim \dot{\phi}(t)$ . As a matter of fact, various choices of parameters  $\Theta$  and  $\lambda_L$ , should not drastically influence to the final results. The numerical solutions of Eq.(2) allows one to obtain the intensity fluctuations defined by Eq.(7). The numerical results of Eq.(7) are plotted by dotted and solid curves in Fig. 5. In resonant case, dynamics of two modes are in phase i.e., well synchronized. The dephasing rate for both cases are chosen to be much smaller than decay rates. Absolute values of two Rabi frequencies are the same as is considered in the experiment. If two-photon detuning  $\Delta$  becomes comparable to  $\gamma_3$  then dynamical behaviors are absolutely out of phase. It is seen more clearly from Fig. 6. Dynamical features shown in Fig. 5, can be seen more clearly in terms of cross correlation functions. Figure 6 describes a switching between two completely different behaviors, namely, correlation and anti-correlation of two modes.

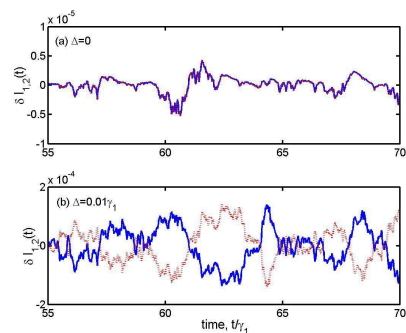


FIG. 5: Synchronized dynamics for intensity differences of two fields (dotted and solid curves) given by Eq.(7) are depicted for resonant (above figure,  $\Delta = 0$ ) and non-resonant (bottom figure,  $\Delta = 0.01\tilde{\gamma}_1$ ) cases. All rates and Rabi frequencies are taken to be  $\tilde{\gamma}_{12,21} = 0.01\tilde{\gamma}_1$ ,  $\tilde{\gamma}_{13,31} = \tilde{\gamma}_3 = 0$ ,  $\tilde{\gamma}_1 = \tilde{\gamma}_2$  and  $\Omega_1 = \Omega_2 = \tilde{\gamma}_1$

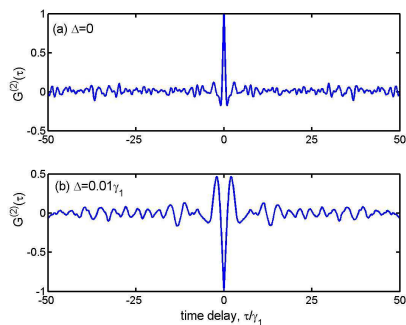


FIG. 6: A perfect photon correlation (a spike at  $\tau = 0$ , see, (a)) for  $\Delta = 0$  and an anti-correlation of two modes (a dip at  $\tau = 0$ , see, (b)) between two modes for  $\Delta = 0.01\tilde{\gamma}_1$  are obtained. The plots are calculated for the same parameters as in Fig. 5.

#### IV. A DECOHERENCE RATE DETERMINED BY SWITCHING IN INTENSITY-INTENSITY CORRELATIONS

In what follows, we analyze this switching in more detail. Similarly as in [28], we focus on correlation functions with zero time delay  $G^{(2)}(\tau = 0)$ . First of all, Eq.(8) is obtained for fixed  $\Omega_1$  but, different  $\gamma_3$  and shown in Fig. 7. Note that transitions from correlated photons to anti-correlated ones are appeared to be smooth and have certain widths. These widths are getting more wide with the increase of dephasing rates. Surprisingly, as shown in Fig. 8, the widths are 'invariant' as functions of re-scaled detuning variable  $\Delta/\gamma_3$  with respect to the corresponding decoherence rates  $\gamma_3$ . Moreover, let us test also how a Rabi frequency's change might affect to correlations. In Fig. 9, we depict numerical results for Eq.(8) depending on not only detuning, but also, Rabi frequencies for two different fixed values of  $\gamma_3$ . As a matter of fact, the corre-

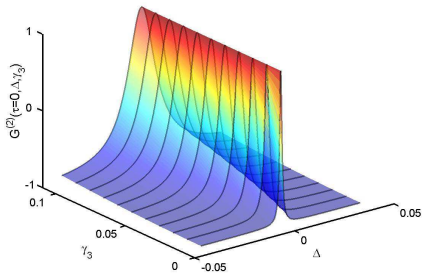


FIG. 7: 3D plot for correlation  $G^{(2)}(\tau = 0, \Delta, \gamma_3)$  with zero time delay ( $\tau = 0$ ) as a function of detuning  $\Delta$  and decoherence rate  $\gamma_3$ . Rabi frequencies are  $\Omega_1 = \Omega_2 = \tilde{\gamma}_1$ .

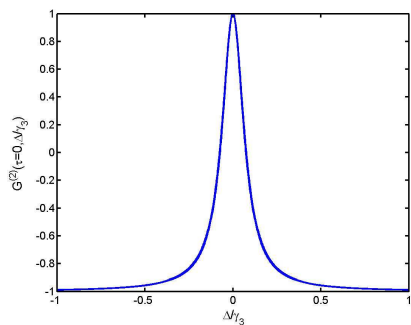


FIG. 8: A sample of correlation functions  $G^{(2)}(\tau = 0, \Delta/\gamma_3)$  with scaled variable as  $\Delta/\gamma_3$  for different decoherence rates:  $\gamma_3 = 0.01, 0.02, \dots, 0.11\tilde{\gamma}_1$ . All curves coincide. The plots are calculated for the parameters taken from Fig. 6.

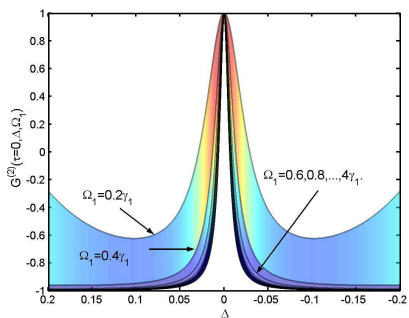


FIG. 9: 2D view of 3D plot for correlation  $G^{(2)}(\tau = 0, \Delta, \Omega_1)$  depending on different values of both detuning and Rabi frequency for fixed dephasing rate  $\gamma_3 = 0.1\tilde{\gamma}_1$ .

lation curves are again 'invariant' for all Rabi frequencies those being not smaller  $\Omega_1 \geq \tilde{\gamma}_1$ . These two intriguing results for the correlation functional invariance do promise a relatively precise determination of the decoherence rate in the robust way from the experimental point of view. As is mentioned in the introduction, the atomic energy

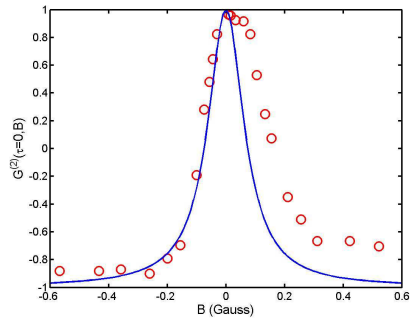


FIG. 10: A finding dephasing rate in Rb vapor. Correlation  $G^{(2)}(\tau = 0, B)$  varying with magnetic field strength  $B$  is compared to the experimental data which allows us to get scaling factor being  $\alpha \sim 1[G]$ . Dephasing rate is, thus, found to be  $\gamma_3 \sim 1\text{MHz}$  independently from  $\tilde{\gamma}_1$ . No free parameters are used here. Experimental data is presented by circles for optical power  $1mW$

levels are perturbed, due to the interaction of the magnetic moments of atoms with the external magnetic field  $B$ . This leads to a non-degeneracy of atomic ground levels. This shift is given by

$$\Delta = aB \quad (15)$$

The constant is defined by Bohr's magneton, the magnetic quantum numbers and gyromagnetic factor as  $a = (\mu_B/\hbar)g(m_2 - m_1)$ . To be more explicit, let us concentrate on  $^{87}\text{Rb}$  vapor in connection to our experiment [28]. An external-cavity diode laser is tuned to  $5S_{1/2}(F = 2) \leftrightarrow 5P_{1/2}(F' = 1)$ . Applied magnetic field leads approximately to three level  $\Lambda$  atomic configuration with a common upper level  $5P_{1/2}(F' = 1, m_3 = 0)$  and two lower levels  $5S_{1/2}(F = 2, m_1 = -1)$  and  $5S_{1/2}(F = 2, m_2 = +1)$ . Using the facts that  $g = 0.5$  for  $S_{1/2}(F = 2)$  and  $\mu_B/\hbar = 1.4\text{MHz}$ , the constant would be estimated  $a = 1.4\text{MHz/G}$ . Moreover, from Eq.(15), the relation for  $B$  can be rewritten as

$$B = \alpha \frac{\Delta}{\gamma_3} \quad (16)$$

where  $\alpha$  is a scaling factor. For fixed  $\alpha$ , all correlations with no time delay are supposed to be invariant. As is seen from Fig. 10, experimental data (circles) are form preserved and have the identical widths regardless of optical powers choices. Asymmetry with respect to the zero detuning may be due to Stark shift which is not of interest in the present situation. Because of two conditions of invariance, there is a very good reason to believe that a form of theoretical correlation functions for all  $\Omega_1 \gg \tilde{\gamma}_1$  and any of  $\gamma_3$ , should be equivalent to the experimental data measured for particular  $\Omega_{exp}$  and  $\gamma_{3exp}$ . In this spirit, theoretical curves by changing scale  $\alpha$ , can be compared with the measurements. Remember that  $\alpha = \gamma_{3exp}/a$ , a new formula for dephasing rate can be

given as

$$\gamma_{3exp} = \alpha a \quad (17)$$

Once  $\alpha$  could be found from experimental data, the dephasing rate for that atomic vapor, is determined by formula Eq.(17). As we expected this is also independent from population decay rates. For Rb vapor, we have found from Fig. 10, that scaling factor  $\alpha \sim 1[G]$ . Therefore, the decoherence rate is estimated to be  $\gamma_{3exp} \sim 1$  MHz.

## V. CONCLUSION

An experimental demonstration of intensity correlations and anti-correlations of coupled fields in a dense Rb vapor is reported. A lower level coherence is created between Zeeman sub-levels by two laser beams with orthogonal circular polarizations. Intensity fluctuations induced by resonant medium are correlated under resonance EIT condition and anti-correlated in presence of non-zero two photon detuning. A narrow correlation peak and anti-correlation dip, in time domain, are associated with frequencies above EIT width and natural optical width. A dependence of correlations on magnetic field (two-photon detuning) show resonance behavior. The resonances are near 4 times narrower than the width of the observed EIT resonances. A smooth transition from perfect correlations to anti-correlations (at zero delay time) between the outgoing beams as functions of the magnetic field strength is robust with respect to a variety of different choices of physical parameters involved and, thus, can provide us with the desired information about decoherence in three level atomic vapor. Moreover, correlation properties of coupled fields in  $\Lambda$  scheme can be used to reduce noise and improve performance of EIT based atomic clocks and magnetometers. The phase noise to intensity noise conversion is an important physical process limiting the accuracy. In EIT atomic clock and magnetometers [42, 43, 44], it is possible to avoid the contribution of the atomic medium induced excess intensity noise.

## Acknowledgements

The authors thank to S.E. Harris, R. Glauber, L.V. Keldysh, A. Muthukrishnan, A. Patnaik, Z.E. Sariyanni, A.V. Sokolov, A.S. Zibrov, I. Novikova, L. Davidovich for useful and fruitful discussions, V.V. Vasiliev for his help with external cavity laser, H. Chen for his help in experiment and gratefully acknowledge the support from the Office of Naval Research under Award No. N00014-03-1-0385, the Air Force Research Laboratory (Rome, NY), Defense Advanced Research Projects Agency-QuIST, Texas A&M University Telecommunication and Information Task Force (TITF) Initiative, and the Robert A. Welch Foundation (Grant No. A-1261).

## Appendix: Stochastic averaging of equations with multiplicative noise

A stochastic average of an arbitrary dynamical variable  $F(x)$ , i.e., a path-integral over all possible realizations of the random numbers  $x(t)$ , is given by

$$\overline{F(x)} = \int D\mu[x] F(x)$$

A white noise does satisfy the relations  $\overline{x(t)} = 0$  and  $\overline{x(t)x(s)} = \Gamma\delta(t-s)$ . A functional measure  $D\mu[x]$  has a Gaussian density

$$D\mu[x] = N^{-1} Dxe^{-\frac{1}{2\Gamma} \int d\tau x(\tau)^2}$$

here  $N$  is normalization coefficient to assure

$$\int D\mu[x] = 1$$

A characteristic function is found to be

$$Z(g) = \overline{e^{i \int d\tau x(\tau)g(\tau)}} = e^{-\frac{\Gamma}{2} \int d\tau g(\tau)^2} \quad (18)$$

Following Wódkiewicz [41], let us consider the following stochastic equations

$$\frac{d\Psi}{dt} = M_0\Psi + ix(t)M\Psi$$

In the interaction picture where  $\Psi_I(t) = e^{-M_0 t}\Psi(t)$ , the equation can be rewritten as

$$\frac{d\Psi_I}{dt} = ix(t)M_I(t)\Psi_I \quad (19)$$

where  $M_I(t) = e^{-M_0 t} M e^{M_0 t}$ . A formal solution of Eq.(19) is given by

$$\Psi_I(t) = T e^{i \int_0^t d\tau x(\tau) M_I(\tau)} \Psi_I(0)$$

here  $T$  is the time ordering operator. Using the relation Eq.(18), the stochastic average to be read

$$\begin{aligned} \overline{\Psi_I(t)} &= \overline{T e^{i \int_0^t d\tau x(\tau) M_I(\tau)} \Psi_I(0)} \\ &= T e^{-\frac{\Gamma}{2} \int_0^t d\tau M_I(\tau)^2} \Psi_I(0) \end{aligned}$$

This is equivalent to the equation

$$\frac{d\overline{\Psi_I}}{dt} = -\frac{\Gamma}{2} M_I(t)^2 \overline{\Psi_I} \quad (20)$$

and, finally, we arrive at

$$\frac{d\overline{\Psi}}{dt} = M_0 \overline{\Psi} - \frac{\Gamma}{2} M^2 \overline{\Psi}. \quad (21)$$

This is the expected stationary equation.

\* e-mail: goa@physics.tamu.edu

- 
- [1] M.O. Scully and S. Zubairy, *Quantum Optics* (Cambridge University Press, Cambridge, 1997).
- [2] R. Hanbury-Brown and R.Q. Twiss, *Nature* **177** 27 (1956).
- [3] R.J. Glauber, *Phys. Rev. Lett.* **130** 2529 (1963).
- [4] H.J. Carmichael and D.F. Walls, *J. Phys. B* **9** 1199 (1976).
- [5] H.J. Kimble, M. Dagenais and L. Mandel, *Phys. Rev. Lett.* **39** 691 (1977).
- [6] H.J. Kimble and L. Mandel, *Phys. Rev. A* **13** 2123 1976; see also: L. Mandel and E. Wolf, *Optical Coherence and Quantum Optics* (Cambridge University Press, Cambridge, 1999).
- [7] G.S. Agarwal, *Phys. Rev. A* **37** 1383 (1976); H.J. Kimble and L. Mandel, *ibid.* **A 15** 689 1977; G.S. Agarwal, *ibid.* **18** 1490 (1978); W. Vogel, D.-G. Welsch and K. Wódkiewicz, *ibid.* **28** 1543 (1983).
- [8] G.S. Agarwal and S.S. Jha, *Z. Physik B* **35** 391 (1979).
- [9] D.A. Braje, V. Balić, S. Goda, G.Y. Yin and S.E. Harris, *Phys. Rev. Lett.* **93** 183601 (2004).
- [10] S.E. Harris, *Phys. Today* **50** 36 (1997); O.A. Kocharovskaya and Y.I. Khanin, *JETP Lett.* **48** 630 (1988).
- [11] V. Balić, D.A. Braje, P. Kolchin, G.Y. Yin and S.E. Harris, *Phys. Rev. Lett.* **94** 183601 (2005).
- [12] A. Kuzmich, W.P. Bowen, A.D. Boozer, A. Boca, C.W. Chou, L.M. Duan, H.J. Kimble, *Nature* **423** 731 (2003).
- [13] C.H. van der Wal, M.D. Eisaman, A. Andre, R.L. Walsworth, D.F. Phillips, A.S. Zibrov, M.D. Lukin, *Science* **301**, 196 (2003).
- [14] see e.g., I.L. Chuang and M.A. Nielsen *Quantum Computation and Quantum Information* (Cambridge University Press, Cambridge, 2000).
- [15] L.-M. Duan, M.D. Lukin, J.I. Cirac and P. Zoller, *Nature* **414** 413 (2001)
- [16] H. Xiong, M.O. Scully and M.S. Zubairy, *Phys. Rev. Lett.* **94** 023601 (2005); M.O. Scully, *ibid.* **55** 2802 (1985); M.O. Scully and M.S. Zubairy, *Phys. Rev. A* **35** 752 (1987), W. Schleich, M.O. Scully and H.-G. von Garssen, *ibid.* **37** 3010 (1988); W. Schleich and M.O. Scully, *ibid.* **37** 1261 (1988).
- [17] U. Rathe and M. Scully, *Lett. Math. Phys.* **34** 297 (1995); M.O. Scully, U.W. Rathe, C. Su and G.S. Agarwal, *Opt. Commun.* **136** 39 (1997).
- [18] M.O. Scully and C.H.R. Ooi, *Quantum Semiclass. Opt.* **6** s816 (2004).
- [19] G.S. Agarwal, G.O. Ariunbold, J. von Zanthier and H. Walther, *Phys. Rev. A* **70** 063816 (2004); G.S. Agarwal, J. von Zanthier, C. Skornia and H. Walther, *Phys. Rev. A* **64**, 063801 (2002).
- [20] M. Hennrich, A. Kuhn and G. Rempe, *Phys. Rev. Lett.* **94** 053604 (2005).
- [21] H.J. Carmichael, P. Drummond, P. Meystre and D.F. Walls *J. Phys. A* **11** (1978).
- [22] S.E. Harris *Phys. Rev. Lett.* **70**, 552 (1993).
- [23] G.S. Agarwal, *Phys. Rev. Lett.* **71**, 1351 (1993)
- [24] A. Beige and G.C. Hegerfeldt *Phys. Rev. A* **58** 4133 (1998).
- [25] A.J. Berglund, A.C. Doherty and H. Mabuchi, *Phys. Rev. Lett.* **89** 068101 (2002); G.O. Ariunbold, G.S. Agarwal, Z. Wang, M.O. Scully and H. Walther, *J. Phys. Chem. A* **108** 2402 (2004).
- [26] C.G. Alzar, L. Cruz, J.A. Gomez, M.F. Santos and P. Nussenzeig, *Europhys. Lett.* **61**, 485 (2003).
- [27] K. Motomura, M. Tsukamoto, A. Wakiyama, K. Harada and M. Mitsunaga, *Phys. Rev. A* **71** 043817 (2005).
- [28] V.A. Sautenkov, Yu.V. Rostovtsev, and M.O. Scully, *Phys. Rev. A* **72**, 065801 (2005).
- [29] T. Yabuzaki, T. Mitsui and U. Tanaka, *Phys. Rev. Lett.* **67** 2453 (1991).
- [30] R. Walser and P. Zoller, *Phys. Rev. A* **49** 5067 (1994).
- [31] D.H. McIntyre, C.E. Fairchild, J. Cooper and R. Walser, *Opt. Lett.* **18**, 1816 (1993).
- [32] J.C. Camparo, *JOSA B*, **15**, 1177 (1998); J.C. Camparo and J.G. Coffer, *Phys. Rev. A* **59**, 728 (1999).
- [33] M. Bahoura and A. Clairon, *Opt. Lett.* **26**, 926, (2001).
- [34] M. Martinelli, P. Valente, H. Failache, D. Felinto, L.S. Cruz, P. Nussenzeig and A. Lezama, *Phys. Rev. A* **69** 043809 (2004).
- [35] V.V. Vassiliev, S.A. Zibrov, V.L. Velichansky, *Rev. Sci. Instrum.* **77**, 013102 (2006)
- [36] A.M. Akulshin, V.A. Sautenkov, V.L. Velichansky, A.S. Zibrov and M.V. Zverkov, *Opt. Commun.* **77** 295 (1990)
- [37] P.A. Roos, S.K. Murphy, L.S. Meng, J.L. Carlsten, T.C. Ralph, A.G. White and J.K. Brasseur, *Phys. Rev. A* **68** 013802 (2003)
- [38] C.W. Gardiner and P. Zoller, *Quantum Noise* (Springer-Verlag, Berlin, 2000)
- [39] G.E. Uhlenbeck and L.S. Ornstein, *Selected papers on Noise and Stochastic Processes*, ed. N. Wax, (Dover Publications, New York, 1954); N.G. van Kampen, *Stochastic Processes in Physics and chemistry* (North-Holland, Amsterdam, 1981).
- [40] R.F. Fox, I.R. Gatland, G. Vemuri, *Phys. Rev. A* **38** 5938 (1988).
- [41] K. Wódkiewicz, *J. Math. Phys.* **20** 45 (1979)
- [42] M. Fleishhauer and M.O. Scully, *Phys. Rev. A* **49**, 1973 (1994).
- [43] J. Kitching, S. Knappe and L. Hollberg, *Appl. Phys. Lett.* **81**, 553 (2002); P.D.D. Schwindt, S. Knappe, V. Shah, L. Hollberg and J. Kitching, *Appl. Phys. Lett.*, **85**, 6409, (2004).
- [44] D. Budker, W. Gawlik, D.F. Kimball, S.M. Rochester, V.V. Yashchuk and A. Weis, *Rev. Mod. Phys.* **74** 1153 (2002).